

ELECTRONIC AND STRUCTURAL PROPERTIES OF C_{36} MOLECULE

XIAOQING YU^{*,†,§}, CONGJUN WU^{*,‡}, CHUI-LIN WANG[†] and ZHAO-BIN SU[†]

^{*}*Department of Physics, Peking University, Beijing 100871, China*

[†]*China Center of Advanced Science and Technology (World Laboratory),
P. O. Box 8730, Beijing, 100080, China*

[‡]*Institute of Theoretical Physics, Chinese Academy of Science,
P. O. Box 2735, Beijing 100080, China*

Received 11 April 1999

The extended SSH model and Bogoliubov–de–Gennes (BdeG) formalism are applied to investigate the electronic properties and stable lattice configurations of C_{36} . We focus the problem on the molecule's unusual D_{6h} symmetry. The electronic part of Hamiltonian without Coulomb interaction is solved analytically. We found that the gap between HOMO and LUMO is small due to the long distance hopping between the 2nd and 5th layers. The charge densities of HOMO and LUMO states are mainly distributed in the two layers, that causes a large splitting between the spin triplet and singlet excitons. The differences of bond lengths, angles and charge densities among molecule and polarons are discussed.

1. Introduction

Recently, a new member of fullerenes, C_{36} , was synthesized by arc-discharge method and purified in bulk quantities.¹ Up to now, it is the smallest fullerene ever discovered. The C_{36} molecule is more curved than C_{60} because of the adjacent pentagonal rings and the small number of carbon atoms.¹ This feature suggests stronger electron–phonon interaction and possible higher superconducting transition temperatures in the alkali-doped C_{36} solids than those of C_{60} .² The Solid-State Nuclear Magnetic Resonant experiment suggested that the most favorable configuration of C_{36} molecule has D_{6h} symmetry.¹ This confirmed the results of the early *ab initio* pseudopotential density functional calculations,³ which indicated that the D_{6h} structure is one of the two most energetically favorable structures among several possibilities.

Looked in a direction perpendicular to the six-fold principal axis (Fig. 1), the molecule is composed of six parallel layers. On each layer, six carbon atoms lie at

[§]Mailing address: China Center of Advanced Science and Technology (World Laboratory), P. O. Box 8730, Beijing, 100080, China. E-mail: xqyu@hp.ccast.ac.cn

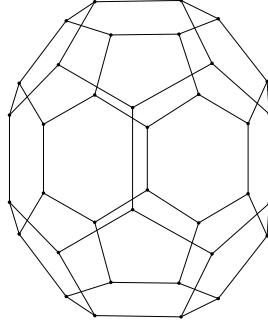


Fig. 1. The geometrical figure of C_{36} molecule.

the vertexes of a hexagon. The edges of the hexagons of the 1st, 2nd, 5th, 6th layers are parallel, while those of the two hexagons in the middle two layers are turned by an angle of 30° . In addition to this special structure, the six-fold principal axis is distinct from the ordinary five-fold principal axis in the cases of C_{60} and C_{70} and little attention has been paid to it. In this paper, we discuss both electronic and structural properties of C_{36} molecule, emphasizing the interesting properties brought by the unusual D_{6h} symmetry.

We employ a simple and elegant model, an extended SSH model, which was successful in treating C_{60} and C_{70} .^{4,5} The BdeG formalism is performed to obtain the stable lattice configuration and the corresponding electronic states self-consistently. The electronic part of Hamiltonian without Coulomb interaction can be solved analytically by methods of group theory. We found that the electron densities of HOMO(B_{1u}) and LUMO(B_{2g}) states, are zero at the two middle layers. Furthermore, the HOMO and LUMO electrons are mainly confined in the 2nd and 5th layers with a possibility of 90%. The gap between them is considerably small, compared to that of C_{60} and C_{70} , because the splitting of HOMO and LUMO is caused by a long-distance hopping in our case. We found the large splitting of the triplet and singlet excitons due to more localized HOMO and LUMO in comparison with C_{60} and C_{70} . As a result, the triplet exciton's energy is very small, and possible experiments are suggested to test this phenomenon.

The geometrical figures of C_{36} molecule and polarons are discussed and bond lengths and angles are calculated. The charge densities on each layer are given. We found that the differences of charge densities among polarons and molecule are mainly in the 2nd and 5th layers.

The following sections are arranged as follows: in Sec. 2, an extended SSH model is introduced; in Sec. 3, we analytically solve the electronic part of the Hamiltonian without Coulomb interaction; in Sec. 4, the whole Hamiltonian is solved self-consistently; in Sec. 5, results and discussions are presented; and conclusions are made in the final section.

2. Model

The Hamiltonian of the extended SSH model to the C₃₆ molecule is written as

$$H = H_0 + H_{\text{int}} + H_{\text{elas}}. \quad (1)$$

The first term H_0 of Eq. (1) is a hopping term of π -electrons,

$$\begin{aligned} H_0 = & - \sum_{\langle i,j \rangle} [t_0 - \alpha(l_{ij} - l_0)](c_{i\sigma}^\dagger c_{j\sigma} + \text{H.c.}) - \sum'_{\langle i,j \rangle} t_1 (c_{i\sigma}^\dagger c_{j\sigma} + \text{H.c.}) \\ & - \sum''_{\langle i,j \rangle} t_2 (c_{i\sigma}^\dagger c_{j\sigma} + \text{H.c.}), \end{aligned} \quad (2)$$

where the three terms describe hoppings between the nearest neighbors, the next nearest neighbors and the third neighbors respectively, with the corresponding hopping integrals t_0 , t_1 and t_2 . The influence of electron-phonon coupling is only included in the first term of H_0 , since those of the last two terms are much smaller than the first term. The third term is important here because it breaks the accidental degeneracy of HOMO and LUMO states, that will be explained in the next section. The larger distance terms are neglected, as they are small and do not bring any new physics.

The second term of Eq. (1) is the screened Coulomb interaction represented by the Hubbard model,

$$H_{\text{int}} = U \sum_i n_{i\uparrow} n_{i\downarrow} + V \sum_{\langle i,j \rangle, \sigma, \sigma'} n_{i\sigma} n_{j\sigma'}, \quad (3)$$

where U is the strength of the on-site interaction, and V is that between the nearest neighbors.

The third term of Eq. (1) is the elastic energy of the lattice. This term is composed of three parts,

$$H_{\text{elas}} = \frac{1}{2} K_1 \sum_{\langle i,j \rangle} (l_{ij} - l_0)^2 + \frac{1}{2} K_2 \sum_i d\theta_{i5}^2 + \frac{1}{2} K_3 \sum_i d\theta_{i6}^2, \quad (4)$$

where the first part describes the spring energy of bond-lengths, and the next two terms describe the spring energy of bond angles. K_i ($i = 1$ to 3) are the elastic constants for these different kinds of lattice vibrations. $d\theta_{i5}$, $d\theta_{i6}$ are bond angle deviations from the original angles 108° , 120° , e.g. $d\theta_{i5} = \theta_{i5} - 108^\circ$. The first summation is taken up over the nearest pairs, while the second is over the interior angles of pentagons, and the third is over the interior angles of hexagons.

Since there are not enough experiment data to determine the semiempirical parameters, we set values in the scope of fullerenes, say C₆₀ and C₇₀, that can produce reasonable results. We adjusted them to obtain the gap between HOMO and LUMO and the bond lengths consistent with those of the pseudopotential density functional approach.² We took $t_0 = 2.5$ eV, $\alpha = 5.6$ eV/Å, $L_0 = 1.55$ Å,

$K_1 = 47 \text{ eV}/\text{\AA}^2$, $K_2 = 8 \text{ eV}/\text{rad}^2$, $K_3 = 7 \text{ eV}/\text{rad}^2$, $t_1 = 0.168t_0$. In fact, the particular values, except for the value of t_2 , would not affect the physics too much. Based on the calculation of the third-nearest π -orbit overlap integral, t_2 was estimated to be $0.111t_0$.

3. Analytical Result Of The Electronic Hamiltonian Without Coulomb Interaction

Fully exploiting the high D_{6h} symmetry, we solve H_0 algebraically as in the case of C_{60} .^{6,7} For simplicity, we temporarily ignore t_1 and t_2 terms and will discuss their effects in detail later. The thirty-six π orbits form a 36×36 representation of the D_{6h} group. It can be reduced into the sum of following irreducible representations:

$$\{3A_{1g} \oplus B_{1g} \oplus 2B_{2g} \oplus 3E_{1g} \oplus 3E_{2g}\} \oplus \{2B_{1u} \oplus 3A_{2u} \oplus B_{2u} \oplus 3E_{1u} \oplus 3E_{2u}\}. \quad (5)$$

The even-order principal axis C_6 brings properties different from those of odd-order principal axis C_5 characterized in C_{60} and C_{70} , in the way that it has 1D representations of kind B.

We reduce this problem by D_{6h} 's subgroup C_{6h} , using quantum numbers $m(= 0, \pm 1, \pm 2, 3)$ and $p(= \pm 1)$ which corresponds to the irreducible representation of C_6 and parity. The thirty-six π orbits are recombined as:

$$|\Psi_{mp}^{(l)}\rangle = \sum_i \eta^{mi} \{|l, i\rangle + p|7-l, i\rangle\}, \quad (6)$$

where $|l, i\rangle$ represents the i th ($i = 1 \sim 6$) carbon atom's π orbit in the l th ($l = 1 \sim 6$) layer. Here l is only ranged from 1 to 3, and $\eta = e^{i\pi/3}$.

The energy eigenstate wavefunction Φ_{mp}^l can be expanded on these basis vectors,

$$\Phi_{mp}^i = \sum_{l=1,3} c_{mp,l}^i \Psi_{mp}^l. \quad (7)$$

Consequently, H_0 can also be reduced to 3×3 matrices in subspace which is spanned by the new bases:

$$H_{mp} = \begin{bmatrix} -t_a(\eta^{-m} + \eta^m) & -t_b & 0 \\ -t_b & 0 & -t_c(1 + \eta^{-m}) \\ 0 & -t_c(1 + \eta^m) & -t_d p \eta^{3m} \end{bmatrix}. \quad (8)$$

Because of the D_{6h} symmetry, there are only four different kinds of bond lengths ($L_a \sim L_d$), see Fig. 2. The corresponding nearest hopping integrals are $t_i = t_0 - \alpha(L_i - L_0)$ ($i = a \sim d$). The energy eigenvalues E_{pm}^l are determined by

$$\lambda^3 + A\lambda^2 + B\lambda + C = 0, \quad (9)$$

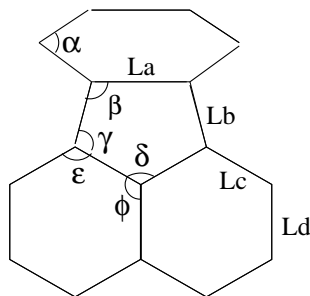


Fig. 2. The bonds and angles of C_{36} molecule.

where

$$A = 2t_a \cos \frac{m\pi}{3} + (-1)^m p t_d,$$

$$B = 2 \cos \frac{m\pi}{3} [(-1)^m p t_a t_d - t_c^2] - (2t_c^2 + t_b^2),$$

$$C = -4 \cos \frac{m\pi}{3} \left(1 + \cos \frac{m\pi}{3}\right) t_a t_c^2 - (-1)^m p t_b^2 t_d.$$

Equation (9) can be solved analytically, so does the eigenvectors. Here we would not list the complicated analytical results. Instead, we present numerical results by using parameter sets, $t_a = 3.30$ eV, $t_b = 2.95$ eV, $t_c = 3.24$ eV, $t_d = 3.08$ eV, that were determined by bond lengths L_i . The coefficients $c_{mp,l}^i$ of the energy eigenstate wavefunction Φ_{mp}^i and the corresponding irreducible representations of D_{6h} are showed in Table 1.

In C_{36} molecule, because hexagons in the two middle layers turn an angle of 30° to the other four hexagons at two ends, the wavefunctions of B_{2u} and B_{1g} energy eigenstates are entirely composed of the atom orbits on the two middle layers, while those of B_{1u} or B_{2g} energy eigenstates only have amplitudes on the other four layers. There are six energy eigenstates of the B kind representations. The 13th(B_{2u}), 22nd(B_{1g}), and the accidentally degenerate 35th(B_{1u}) and 36th(B_{2g}) levels lie either far below or above the Fermi level, so they are out of interest. There are also another pair of accidentally degenerate 18th(B_{1u}) and 19th(B_{2g}) levels which are half filled. We also notice that in Table 1 the 18th(B_{1u}) and 19th(B_{2g}) electrons are distributed in the 2nd and 5th layers with 90% possibility and 10% in the 1st and 6th layers.

When $t_1(0.168t_0)$ and $t_2(0.111t_0)$ are considered, H_{mp} has a different form. The long distance hopping (t_2) coupling the 2nd and 5th layers results in B_{1u} and B_{2g} 's splitting. This is the reason that we introduce much longer distance hopping term than usual. Because the charge densities of B_{1u} and B_{2g} are mainly distributed in the 2nd and 5th layers, the gap between HOMO(B_{1u}) and LUMO(B_{2g})

Table 1. The analytical solution of H_0 without t_1 and t_2 terms.

m, p	$E(\text{eV})$	$c_{mp,1}$	$c_{mp,2}$	$c_{mp,3}$
$0, +(A_{1g})$	-9.51	0.581	0.574	0.578
	-5.74	0.791	-0.232	-0.566
	5.57	0.190	-0.786	0.589
$0, -(A_{2u})$	-8.43	0.816	0.504	0.284
	-3.53	-0.565	0.589	0.578
	8.43	-0.124	0.632	-0.765
$\pm 1, +(E_{1g})$	-6.28	0.647	0.654	$0.340 \pm 0.196i$
	-1.60	0.744	-0.428	$-0.445 \mp 0.257i$
	7.66	$0.145 \mp 0.084i$	$-0.540 \pm 0.312i$	0.763
$\pm 1, -(E_{1u})$	-8.09	$0.329 \mp 0.190i$	$0.534 \mp 0.308i$	0.690
	-3.25	0.882	-0.015	$-0.409 \mp 0.236i$
	4.97	-0.281	0.787	$-0.476 \mp 0.275i$
$\pm 2, +(E_{2g})$	-5.44	$0.096 \mp 0.169i$	$0.289 \mp 0.501i$	0.792
	0.269	0.573	0.589	$-0.285 \mp 0.494i$
	5.40	0.796	-0.565	$0.108 \pm 0.187i$
$\pm 2, -(E_{2u})$	-3.07	0.379	0.819	$0.216 \pm 0.374i$
	3.20	0.727	0.026	$-0.343 \mp 0.595i$
	6.20	$0.287 \mp 0.496i$	$-0.287 \pm 0.497i$	0.585
$3, +(B_{2g})$	-1.13	0.357	0.934	0
$3, +(B_{1g})$	3.08	0	0	1
$3, +(B_{2g})$	7.73	0.934	-0.357	0
$3, -(B_{2u})$	-3.08	0	0	1
$3, -(B_{1u})$	-1.13	0.357	0.934	0
$3, -(B_{2u})$	7.73	0.934	-0.357	0

is approximate to $2t_2$ (≈ 0.5 eV in our parameters). When the electron–electron interaction is taken into account, the electronic Hamiltonian has to be solved in the HF mean field theory with self-consistent method. The energy levels of ground state configuration are shown in Fig. 3. We can see that in Fig. 3 and Table 1, the relative positions of the energy levels only change slightly, except for the splitting of B_{1u} and B_{2g} . In Fig. 3, the separation between the 16th, 17th levels (E_{1g}) and HOMO is about 0.2 eV and that between the 20th, 21st levels (E_{2g}) and LUMO is 1.3 eV.

4. Numerical Scheme

Under the adiabatic approximation, we apply the BdeG formalism to the Hamiltonian to obtain the stable lattice configuration and the corresponding electronic structure. Molecular dynamical procedure is adopted to gradually approach the

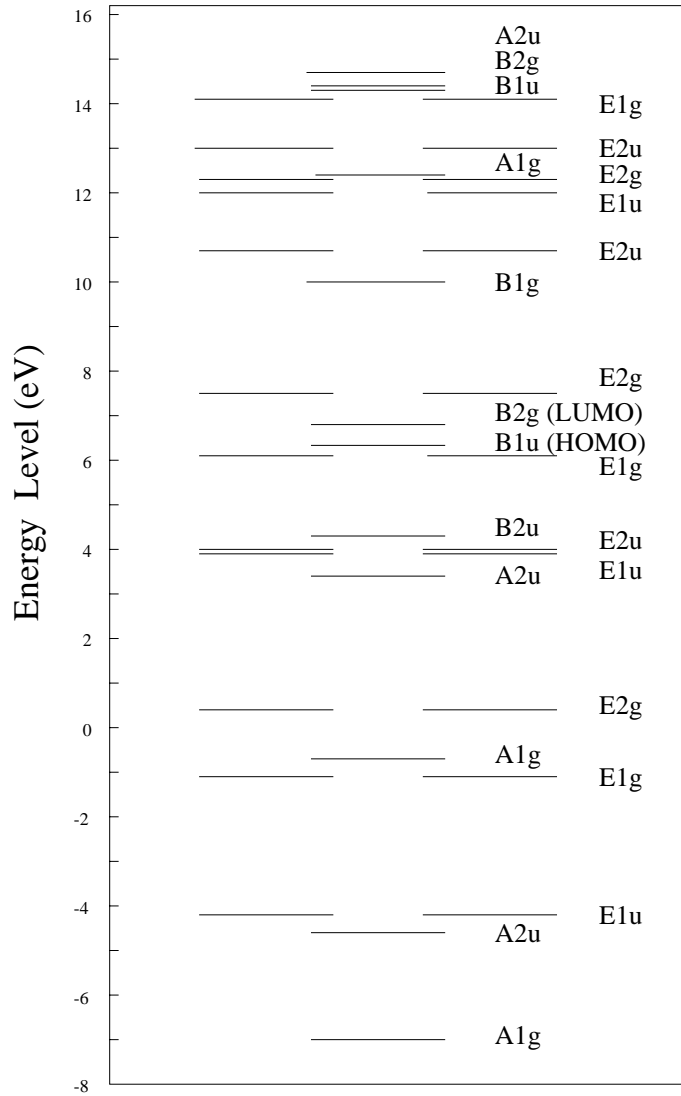


Fig. 3. Energy levels of the ground state C₃₆ molecule.

minimum of the potential surface from an initial lattice configuration. The following two equations are used,

$$F_{i\sigma} = -\frac{dV_{\text{eff}}}{dx_{i\sigma}} \quad (\sigma = 1 - 3), \quad (10)$$

$$v_{i\sigma} = \frac{dx_{i\sigma}}{dt}, \quad (11)$$

where V_{eff} is the effective lattice potential that includes the elastic energy of the lattice and the electron–lattice interaction energy, both of which depend on

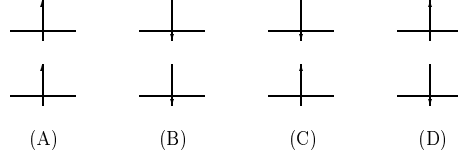


Fig. 4. The four possible configurations of the lowest excitons.

the lattice coordinates. $F_{i\sigma}$ is the σ component of the effective force acting on the i th atom under this potential. $x_{i\sigma}$ is the σ coordinate of the i th atom.

At each step in the dynamical process, we solve the electronic part of the Hamiltonian under the lattice configuration given by the last step. The HF mean field theory is performed to approximate the electron–electron interaction. Then the electronic states and wavefunctions are obtained self-consistently.

$$\begin{aligned}
 H_{\text{MF}}^{\text{el}} = & H_0 + U \sum_i \{ \langle n_{i\uparrow} \rangle n_{i\downarrow} + \langle n_{i\downarrow} \rangle n_{i\uparrow} - \langle n_{i\uparrow} \rangle \langle n_{i\downarrow} \rangle \} \\
 & + V \sum_{\langle i,j \rangle, \sigma, \sigma'} \{ \langle n_{i\sigma} \rangle n_{j\sigma'} + \langle n_{j\sigma'} \rangle n_{i\sigma} - \langle n_{i\sigma} \rangle \langle n_{j\sigma'} \rangle \} \\
 & - V \sum_{\langle i,j \rangle, \sigma} \{ \langle c_{i\sigma}^\dagger c_{j\sigma} \rangle c_{j\sigma}^\dagger c_{i\sigma} + \langle c_{j\sigma}^\dagger c_{i\sigma} \rangle c_{i\sigma}^\dagger c_{j\sigma} - \langle c_{i\sigma}^\dagger c_{j\sigma} \rangle \langle c_{j\sigma}^\dagger c_{i\sigma} \rangle \}. \quad (12)
 \end{aligned}$$

The ground state and the lowest triplet and singlet excitons are investigated. There are four lowest exciton configurations A , B , C and D , see Fig. 4. Due to Coulomb interaction, C and D are mixed to give singlet and triplet,

$$\begin{aligned}
 \langle C | H_{\text{int}} | D \rangle = & - \sum_i U \psi_{\alpha\uparrow}^*(i) \psi_{\beta\downarrow}^*(i) \psi_{\beta\uparrow}(i) \psi_{\alpha\downarrow}(i) \\
 & - V \sum_{\langle ij \rangle} \{ \psi_{\alpha\uparrow}^*(i) \psi_{\beta\downarrow}^*(j) \psi_{\beta\uparrow}(i) \psi_{\alpha\downarrow}(j) \\
 & + \psi_{\alpha\uparrow}^*(j) \psi_{\beta\downarrow}^*(i) \psi_{\beta\uparrow}(j) \psi_{\alpha\downarrow}(i) \}, \quad (13)
 \end{aligned}$$

where α and β denote the 18th and 19th energy level respectively.

5. Results and Discussion

The configurations and energy of ground and low excited states are given below,

$$E_1^{\text{el}} = -64.25 \text{ eV}, \quad |\Phi_1\rangle \quad (\text{spin singlet ground state}), \quad (14a)$$

$$E_2^{\text{el}} = -64.00 \text{ eV}, \quad |\Phi_2^{1\sim 3}\rangle = |A\rangle, |B\rangle, \quad (14b)$$

$$\frac{1}{\sqrt{2}}(|C\rangle + |D\rangle) \quad (\text{spin triplets}),$$

$$E_3^{\text{el}} = -63.37 \text{ eV}, \quad |\Phi_3\rangle = \frac{1}{\sqrt{2}}(|C\rangle - |D\rangle) \quad (\text{spin singlet}). \quad (14c)$$

We can see that the ground state Φ_1 is a spin singlet rather than triplet after the long distance hopping t_2 and electron–electron interaction are considered, that is an improvement of the prediction of simple Hückel theory. And there is no need to add the hybridizing of σ and π bonds to investigate the qualitative physics of C₃₆ as discussed in Ref. 8.

The lowest excited states $\Phi_2^{1\sim 3}$ are spin triplet excitons, which are only about 0.25 eV above the ground state. The energy of singlet exciton Φ_3 is very high, and the splitting between the triplet and singlet excitons is about 0.63 eV, which is much larger than 0.2 eV in the case of C₆₀ and 0.28 eV of C₇₀. This is because the electron densities of HOMO and LUMO are more localized, 90% in the 2nd and 5th layers and 10% in the 1st and 6th layers. Compared to the C₃₆ case, the electron densities of HOMO and LUMO in C₆₀ and C₇₀ are distributed more uniformly over all sites, so the splitting of the singlet and triplet exciton due to the Coulomb interaction is relatively small. The fact that the triplet exciton has low energy can be verified through experiment observation: when illuminated by external light, the C₃₆ might be excited to the state of the singlet exciton and then may transit to the triplet exciton through nonradiative decay. The transition rate to ground state is slow because of the different spin configuration and small energy splitting. We predict that the triplet excitons are metastable states, and the phosphorescence phenomena is possible to be observed. The triplet exciton is paramagnetic, while the ground state is a diamagnetic singlet. So the magnetic susceptibility is increased upon illumination of the external light. Electron Spin Resonance (ESR) experiment can be performed to detect the triplet exciton states. When ESR is performed to a solution sample, the usual unimportant magnetic dipole interaction between electrons becomes crucial because its anisotropy can smear the resonance peak. However, this interaction is decayed rapidly with distance as R^{-3} . The electrons in HOMO and LUMO are mainly uniformly distributed on 12 carbon atoms in the two layers, the possibility of their short distance is considerably small compared to other small organic molecule, such as naphthalene. So the resonance peak will be possibly observed. The photon absorption and luminescence spectra experiments can also be performed to test the lowest singlet exciton's energy.

The shape of the C₃₆ molecule is an ellipsoid with high aspect ratios. Our calculation shows that the distance between the 1st and 6th layers is 5.2 Å, and that between the parallel vertical hexagon planes is 4.2 Å. The charge densities, bond lengths and bond angles of C₃₆ molecule and polarons are calculated and shown in Tables 2, 3 and 4. We note that because of the D_{6h} symmetry of the molecule, the 1st and 6th layers are regular hexagons, with each interior angle 120° and the shortest bonds L_a (1.41 Å). The six vertical hexagons around the equator are slightly deformed due to the pull of the 1st and 6th layers from each side. L_d is 2.8% longer than L_a and 2% than L_c . L_b bonds are relatively weaker than those in hexagons, because they couple the hexagons in the two ends with the hexagons around the equator. L_b is 4.4% longer than L_a . This result is consistent with that of LDA except that L_d is as long as L_c in LDA, and we think that our result is reasonable.

Table 2. The ground state charge density per site on each layer of polarons and neutral molecule.

	1	2	3	4	5	6
C_{36}^{2-}	1.053	1.131	0.991	0.991	1.131	1.053
C_{36}^-	1.042	1.057	0.985	0.985	1.057	1.042
C_{36}	1.031	0.981	0.988	0.988	0.981	1.031
C_{36}^+	1.021	0.902	0.992	0.992	0.902	1.021
C_{36}^{2+}	1.013	0.823	0.997	0.997	0.823	1.013

Table 3. The bond lengths (\AA) of polarons and neutral molecule.

	L_a	L_b	L_c	L_d
SSH(C_{36}^{2-})	1.414	1.453	1.418	1.447
SSH(C_{36}^-)	1.410	1.462	1.418	1.447
SSH(C_{36})	1.407	1.470	1.418	1.447
SSH(C_{36}^+)	1.404	1.477	1.417	1.447
SSH(C_{36}^{2+})	1.402	1.484	1.417	1.448
LDA(C_{36})	1.41	1.48	1.43	1.43

Table 4. The bond angles within SSH model.

	α	β	γ	δ	ϵ	ϕ
C_{36}	120.00°	107.64°	108.20°	108.29°	119.42°	119.24°

The bond lengths of L_c and L_d of polarons differ from those of molecule very slightly. But the negative polarons' L_a is longer and positive polarons' is shorter than neutral molecule's, while the L_b changes in the opposite way. The reason is that the wavefunctions of the electron in the 18th(B_{1u}) and 19th(B_{2g}) levels have opposite sign between two nearest sites connected by L_a , same sign by L_b , and have zero amplitude on the 3rd, 4th layers. According to the contribution of these two states from the hopping term, the sites connected by L_a are repulsive, but those connected by L_b are attractive. The bond angles in the pentagons and hexagons around the equator deviate from 108° and 120° slightly, which justifies the validity of H_{elas} . The bond angles in polarons differ from those of the neutral molecule very slightly, so we omit them in Table 4. Form C_{36}^{2+} polaron to C_{36}^{2-} , the adding electrons distribute mostly in the 2nd and 5th layers. This is because of the particular charge density distribution of the 18th and 19th levels.

6. Conclusion

In this paper, we have carefully studied the effect of D_{6h} symmetry on C_{36} 's electronic properties under the extended SSH model. A small gap between HOMO(B_{2u}) and LUMO(B_{1g}) is obtained due to the long distance hopping. The large splitting of the spin triplet and singlet lowest excitons, the differences of bond lengths and electron density between molecule and polarons are discussed as results brought by more localized HOMO and LUMO states and their unusual symmetries. Possible experiments are suggested.

Acknowledgment

We thank Dr. Xi Dai for his helpful discussions.

References

1. C. Piskoti, J. Yarger and A. Zettl, *Nature* **393**, 771 (1998).
2. M. Côté, J. C. Grossman, S. G. Louie and M. L. Cohen, *Phy. Rev. Lett.* **81**, 697 (1998).
3. J. C. Grossman, M. Côté, S. G. Louie and M. L. Cohen, *Chem. Phys. Lett.* **284**, 344 (1998).
4. W. M. You, C. L. Wang, F. C. Zhang and Z. B. Su, *Phy. Rev.* **B47**, 4765 (1993).
5. L. Tian, Y. S. Yi, C. L. Wang and Z. B. Su, *Int. J. Mod. Phys.* **B11**, 1969 (1997).
6. C. L. Wang, W. Z. Wang and Z. B. Su, *J. Phys. Condes. Matter* **5**, 5581 (1993).
7. Y. Deng and C. N. Yang, *Phys. Lett.* **A170**, 116 (1992).
8. J. R. Heath, *Nature* **393**, 730 (1998).